
**Separation Science and Technology**
Publication details, including instructions for authors and subscription information:
http://www.informaworld.com/smpp/title~content=t713708471

# Modeling and Simulation of Continuous Rotating Annular Ion-Exchange Chromatography for Separation of Amino Acids

Akio Kitakawa[a]; Yoshihito Yamanishi[b]; Toshikuni Yonemoto[b]; Teiriki Tadaki[b]
[a] Miyagi National College Of Technology, Natori, Japan [b] DEPARTMENT OF BIOCHEMISTRY AND ENGINEERING, TOHOKU UNIVERSITY, SENDAI, JAPAN

**To cite this Article** Kitakawa, Akio , Yamanishi, Yoshihito , Yonemoto, Toshikuni and Tadaki, Teiriki(1995) 'Modeling and Simulation of Continuous Rotating Annular Ion-Exchange Chromatography for Separation of Amino Acids', Separation Science and Technology, 30: 16, 3089 — 3110
**To link to this Article: DOI:** 10.1080/01496399508013132
**URL:** http://dx.doi.org/10.1080/01496399508013132

SEPARATION SCIENCE AND TECHNOLOGY, 30(16), pp. 3089–3110, 1995

# Modeling and Simulation of Continuous Rotating Annular Ion-Exchange Chromatography for Separation of Amino Acids

AKIO KITAKAWA
MIYAGI NATIONAL COLLEGE OF TECHNOLOGY
NATORI, JAPAN

YOSHIHITO YAMANISHI, TOSHIKUNI YONEMOTO,* and TEIRIKI TADAKI
DEPARTMENT OF BIOCHEMISTRY AND ENGINEERING
TOHOKU UNIVERSITY
AOBA, ARAMAKI, AOBA-KU, SENDAI 980-77, JAPAN



## ABSTRACT

Separation of an amino acid mixture using continuous rotating annular ion-exchange chromatography is numerically simulated by a newly constructed mathematical model. Dissociation reactions of amino acids and eluent buffer components, Nernst–Planck-type intraparticle ionic transport, and a nonlinear ion-exchange equilibrium based on ion-exchange selectivity are considered in the model. The simulated and the experimental results agree well under various operation conditions. The effects of rotation speed of the annular bed and the interstitial liquid velocity on separation are studied experimentally and theoretically.

## INTRODUCTION

Continuous rotating annular chromatography (CRAC), proposed by Martin (1), Giddings (2), and Fox et al. (3–5), has been applied to the separation and concentration of amino acids (6–8) or proteins (9, 10) combined with an ion-exchange technique. For industrial utilization or rational

* To whom correspondence should be addressed. Telephone: 81-22-217-7255; FAX: 81-22-217-7258.

designing of the apparatus in this method, however, a detailed mathematical model for the separation process is required.

Ion-exchange chromatographic separation of amino acids using CRAC is a complex phenomenon in which the following elemental processes proceed simultaneously:

1. Axial transport in the liquid phase by liquid flow.
2. Circumferential transport in the liquid phase by rotation of the annular bed.
3. Axial and circumferential transports in the liquid phase by dispersion.
4. Dissociation reactions of dissociative species in the liquid phase.
5. Ion-exchange reaction between the liquid and ion-exchange resin phases.
6. Transport in the resin phase by diffusion and electric interaction (migration).
7. Circumferential transport in the resin phase by rotation of the annular bed.

It is desired for the mathematical model to describe all of these processes. In the conventional models, however, some simplifications have been made based on the following assumptions.

- Circumferential transport by dispersion is neglected (9).
- Dissociation reactions are neglected and the concentrations of amino acids in the resin phase are described using linear or power functions of the total concentrations in the liquid phase (7, 8, 10).
- The fluxes in the resin phase are described using Fick's law (7, 8, 10).

By neglecting the circumferential dispersion, the model for CRAC becomes mathematically equivalent to that for conventional column operation and the analysis becomes easier (9). However, it is not physically strict that a one-dimensional (axial) dispersion is used in a two-dimensional packed bed of CRAC (12).

It is also a common procedure to neglect the dissociation reactions and to describe the ion-exchange equilibrium relations using a function of the total concentration alone. However, when the eluent composition is changed, e.g., under pH gradient elution, the dissociation equilibrium of amino acids is shifted and other equilibrium relations should be used (7, 8, 10).

When an ion-exchange resin of comparatively large size is used, the contribution of mass transfer resistance in the resin phase cannot be neglected. The mass transfer fluxes are affected not only by the concentration gradient but also by the electric potential distribution, so that they cannot be described using the simple Fick's law (11).

The authors have constructed a novel mathematical model (13) for the one-dimensional separation process of amino acids using ion-exchange column chromatography based on the following strategies:

- Considering the dissociation reactions of the amino acids and the eluent buffer.
- Describing the ion-exchange relations using nonlinear ion-exchange selectivity.
- Applying the Nernst–Planck equation (11) for the mass transfer fluxes in the resin phase.

The authors have certified its applicability to the changes in feed concentrations of a mixture of amino acids, the flow rate, and composition of the eluent buffer.

In this work we extend the model to two-dimensional separation and apply it to the continuous ion-exchange chromatographic separation of amino acids using the CRAC which had been constructed in the previous study (12). The effects of some operation factors are also elucidated.



## MATHEMATICAL MODELING

### Separation System

Let us consider the separation system of glutamic acid and valine with a sodium acetate buffer eluent and a cation-exchange resin for chromatographic packing (13). In this system the following 12 chemical species exist by following eight dissociation reactions. For glutamic acid,

$$GH_3^+ \rightleftarrows GH_2^0 + H^+; \qquad K_1 = \frac{C_{GH_2^0} C_{H^+}}{C_{GH_3^+}} = 10^{0.81}\ \text{mol/m}^3 \tag{1}$$

$$GH_2^0 \rightleftarrows GH^- + H^+; \qquad K_2 = \frac{C_{GH^-} C_{H^+}}{C_{GH_2^0}} = 10^{-1.25}\ \text{mol/m}^3 \tag{2}$$

$$GH^- \rightleftarrows G^{2-} + H^+; \qquad K_3 = \frac{C_{G^{2-}} C_{H^+}}{C_{GH^-}} = 10^{-6.67}\ \text{mol/m}^3 \tag{3}$$

for valine,

$$VH_2^+ \rightleftarrows VH^0 + H^+; \qquad K_4 = \frac{C_{VH^0} C_{H^+}}{C_{VH_2^+}} = 10^{0.68}\ \text{mol/m}^3 \tag{4}$$

$$VH^+ \rightleftarrows V^- + H^+; \qquad K_5 = \frac{C_{V^-} C_{H^+}}{C_{VH^0}} = 10^{-6.62}\ \text{mol/m}^3 \tag{5}$$

for sodium acetate,

$$NaA \rightarrow Na^+ + A^-; \qquad \text{Complete dissociation} \tag{6}$$

$$HA^0 \rightleftharpoons A^- + H^+; \qquad K_6 = \frac{C_{A^-}C_{H^+}}{C_{HA^0}} = 10^{-1.71}\ \text{mol/m}^3 \tag{7}$$

and for the solvent water,

$$H_2O \rightleftharpoons OH^- + H^+; \qquad K_7 = C_{H^+}C_{OH^-} = K_W = 10^{-8.00}\ \text{mol}^2/\text{m}^6 \tag{8}$$

The meanings of the symbols for the species are listed in Table 1.

## Derivation of Governing Equations

The coordinate system for modeling is shown in Fig. 1. Because the thickness of the annular packed bed is much smaller than its radius, a two-dimensional rectangular coordinate can be used for the liquid phase. $x$ and $y$ correspond to liquid flow and rotation directions, respectively. For the ion-exchange resin phase, a one-dimensional spherical coordinate can be used, with $r$ for the radial direction.

The following assumptions are laid down for the liquid phase:

1. A local dissociation equilibrium is set up.
2. The migration of species due to the electric potential gradient is negligible compared to the convection, rotation, and dispersion.
3. Only the cationic species take part in the ion-exchange reaction.

TABLE 1
List of Species in the System

| Species | Symbol |
|---|---|
| Cationic glutamic acid | $GH_3^+$ |
| Zwitterionic glutamic acid | $GH_2^0$ |
| Anionic glutamic acid (monovalent) | $GH^-$ |
| Anionic glutamic acid (divalent) | $G^{2-}$ |
| Cationic valine | $VH_2^+$ |
| Zwitterionic valine | $VH^0$ |
| Anionic valine | $V^-$ |
| Undissociated acetic acid | $HA^0$ |
| Acetate ion | $A^-$ |
| Hydrogen ion | $H^+$ |
| Hydroxy ion | $OH^-$ |
| Sodium ion | $Na^+$ |

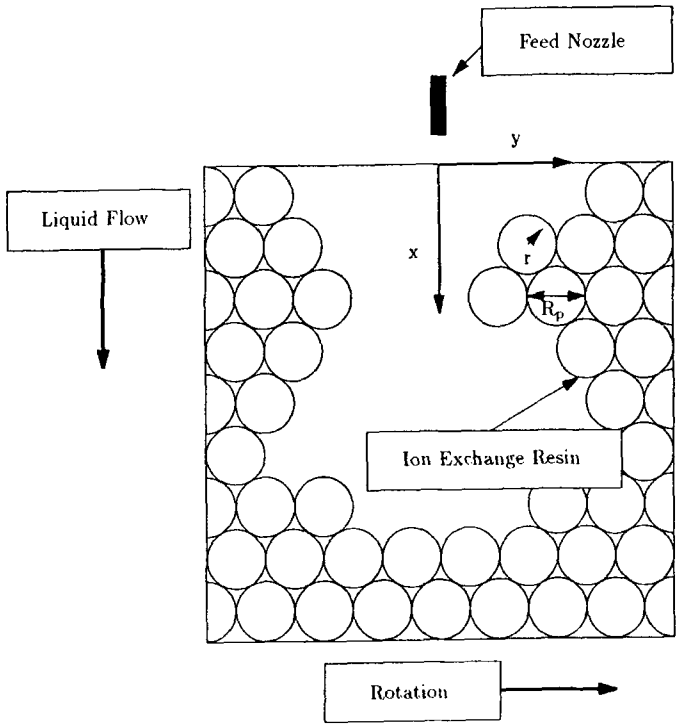


FIG. 1 Coordinate system.



The mass balance equation for glutamic acid in the liquid phase can be given as

$$E_{g,x}\frac{\partial^2 C_{gT}}{\partial x^2} + E_{g,y}\frac{\partial^2 C_{gT}}{\partial y^2} - u\frac{\partial C_{gT}}{\partial x} - u_y\frac{\partial C_{gT}}{\partial y} - Hu_y\frac{\partial \overline{q_{GH_3^+}}}{\partial y} = 0 \quad (9)$$

The subscript gT corresponds to the total concentration of glutamic acid defined as

$$C_{gT} = C_{GH_3^+} + C_{GH^\pm} + C_{GH^-} + C_{G^{2-}} \quad (10)$$

$H$ and $\overline{q_{GH_3^+}}$ are the volume ratio of the liquid and resin phases and the volumetric mean concentration of the cation in the resin phase, respectively, defined as

$$H = \frac{1-\epsilon}{\epsilon} \quad (11)$$

$$\overline{q_{GH_3^+}} = \frac{\int_{V_r} q_{GH_3^+}\, dV}{\int_{V_r} dV} = \frac{3}{R_p}\int_0^{R_p} q_{GH_3^+}\, dr \tag{12}$$

Here, $R_p$ is the radius of the ion-exchange resin.

The terms in Eq. (9) correspond to dispersions in the directions of liquid flow and rotation, transport due to liquid flow, transport due to rotation, and cation exchange with resin phase, respectively. Compared with the mass balance equation for column chromatography (13), the unsteady term disappears, and instead, convection and dispersion terms in the rotational direction appear. The following correspondences exists between them.

$$\text{CRAC} \leftrightarrow \text{column}$$

$$E_{g_y}\frac{\partial^2 C_{gT}}{\partial y^2} \leftrightarrow \text{"not included"} \tag{13}$$

$$u_y\frac{\partial C_{gT}}{\partial y} \leftrightarrow \frac{\partial C_{gT}}{\partial t} \tag{14}$$

$$Hu_y\frac{\partial \overline{q_{GH_3^+}}}{\partial y} \leftrightarrow H\frac{\partial \overline{q_{GH_3^+}}}{\partial t} \tag{15}$$

The term for dispersion in the rotational direction comes from the fact that the packed bed of CRAC is two-dimensional; there is no corresponding term in column chromatography. The relationship between $t$ and $y$ is as follows:

$$t = y/u_y \tag{16}$$

For valine and sodium ion, the following equations can be written in the same manner.

$$E_{v,x}\frac{\partial^2 C_{vT}}{\partial x^2} + E_{v,y}\frac{\partial^2 C_{vT}}{\partial y^2} - u\frac{\partial C_{vT}}{\partial x} - u_y\frac{\partial C_{vT}}{\partial y} - Hu_y\frac{\partial \overline{q_{VH_3^+}}}{\partial y} = 0 \tag{17}$$

$$C_{vT} = C_{VH_3^+} + C_{VH^0} + C_{V^-} \tag{18}$$

$$\overline{q_{VH_2^+}} = \frac{3}{R_p}\int_0^{R_p} q_{VH_2^+}\,dr \tag{19}$$

$$E_{Na^+,x}\frac{\partial^2 C_{Na^+}}{\partial x^2} + E_{Na^+,y}\frac{\partial^2 C_{Na^+}}{\partial y^2} - u\frac{\partial C_{Na^+}}{\partial x} - u_y\frac{\partial C_{Na^+}}{\partial y} - Hu_y\frac{\partial \overline{q_{Na^+}}}{\partial y} = 0 \tag{20}$$

$$\overline{q_{Na^+}} = \frac{3}{R_p}\int_0^{R_p} q_{Na^+}\,dr \tag{21}$$

For acetic acid, the following equations are given because it does not participate in the cation exchange.

$$E_{a,x}\frac{\partial^2 C_{aT}}{\partial x^2} + E_{a,y}\frac{\partial^2 C_{aT}}{\partial y^2} - u\frac{\partial C_{aT}}{\partial x} - u_y\frac{\partial C_{aT}}{\partial y} = 0 \tag{22}$$

$$C_{aT} = C_{HA^0} + C_{A^-} \tag{23}$$

The concentrations of ionic species in the liquid phase are under the restriction of electroneutrality as

$$C_{GH_3^+} + C_{VH_2^+} + C_{H^+} + C_{Na^+} = C_{GH^-} + 2C_{G^{2-}} + C_{V^-} + C_{A^-} + C_{H^+} \tag{24}$$

Using dissociation equilibrium relations and Eq. (24), the following equation can be obtained:

$$\frac{C_{gT}(C_{H^+}^3 - K_1K_2C_{H^+} - 2K_1K_2K_3)}{C_{H^+}^3 + K_1C_{H^+}^2 + K_1K_2C_{H^+} + K_1K_2K_3} + \frac{C_{vT}(C_{H^+}^2 - K_4K_5)}{C_{H^+}^2 + K_4C_{H^+} + K_4K_5} - \frac{C_{aT}K_6}{C_{H^+} + K_6} + C_{H^+} - \frac{K_W}{C_{H^+}} + C_{Na^+} = 0 \tag{25}$$

The concentration of hydrogen ion can be calculated using Eq. (25).

The following assumptions are laid down for the resin phase:

4. The radius of the ion-exchange resin particle is constant.
5. The intraparticle diffusion coefficient of each ion is constant.
6. Dissociation reactions do not occur in the resin phase.

The mass transfer flux of each cation in the resin phase can be written using the Nernst–Planck equation as

$$\overline{j_{GH_3^+}} = \overline{D_{GH_3^+}}\left(\frac{\partial q_{GH_3^+}}{\partial r} + q_{GH_3^+}\frac{\mathcal{F}}{\mathcal{R}\mathcal{T}}\frac{\partial \psi}{\partial r}\right) \tag{26a}$$

$$\overline{j_{VH_2^+}} = \overline{D_{VH_2^+}} \left( \frac{\partial q_{VH_2^+}}{\partial r} + q_{VH_2^+} \frac{\mathcal{F}}{\mathcal{R}\mathcal{T}} \frac{\partial \psi}{\partial r} \right) \tag{26b}$$

$$\overline{j_{H^+}} = \overline{D_{H^+}} \left( \frac{\partial q_{H^+}}{\partial r} + q_{H^+} \frac{\mathcal{F}}{\mathcal{R}\mathcal{T}} \frac{\partial \psi}{\partial r} \right) \tag{26c}$$

$$\overline{j_{Na^+}} = \overline{D_{Na^+}} \left( \frac{\partial q_{Na^+}}{\partial r} + q_{Na^+} \frac{\mathcal{F}}{\mathcal{R}\mathcal{T}} \frac{\partial \psi}{\partial r} \right) \tag{26d}$$

The second term in the parenthesis in each equation corresponds to the migration due to the electric potential gradient.

The concentrations of cations in the resin are restricted by the following electroneutrality condition.

$$q_{GH_3^+} + q_{VH_2^+} + q_{H^+} + q_{Na^+} = Q \tag{27}$$

Here, $Q$ is the ion-exchange capacity of a resin.

Because there is no net electric current in the resin, the following equation is valid:

$$\overline{j_{GH_3^+}} + \overline{j_{VH_2^+}} + \overline{j_{H^+}} + \overline{j_{Na^+}} = 0 \tag{28}$$

Combining Eqs. (26) to (28) and eliminating the concentration gradient of hydrogen ion gives:

$$\overline{j_{GH_3^+}} = \sum_{\mu = GH_3^+, VH_2^+, Na^+} \overline{D_{GH_3^+, \mu}} \frac{\partial q_\mu}{\partial r} \tag{29a}$$

$$\overline{j_{VH_2^+}} = \sum_{\mu = GH_3^+, VH_2^+, Na^+} \overline{D_{VH_2^+, \mu}} \frac{\partial q_\mu}{\partial r} \tag{29b}$$

$$\overline{j_{Na^+}} = \sum_{\mu = GH_3^+, VH_2^+, Na^+} \overline{D_{Na^+, \mu}} \frac{\partial q_\mu}{\partial r} \tag{29c}$$

Here, $\overline{D_{\lambda,\mu}}$ is the effective diffusion coefficient, defined as

$$\overline{D_{\lambda,\mu}} = \begin{cases} -\dfrac{\overline{D_\lambda}\,(\overline{D_\mu} - \overline{D_{H^+}})\, q_\lambda}{\sum_{\nu = GH_3^+, VH_2^+, H^+, Na^+} \overline{D_\nu} q_\nu} & (\lambda \neq \mu) \\ \overline{D_\lambda} - \dfrac{\overline{D_\lambda}\,(\overline{D_\lambda} - \overline{D_{H^+}})\, q_\lambda}{\sum_{\nu = GH_3^+, VH_2^+, H^+, Na^+} \overline{D_\nu} q_\nu} & (\lambda = \mu) \end{cases} \tag{30}$$

The mass balance of cationic glutamic acid in the resin phase can then be obtained as follows:

$$u_y \frac{\partial \overline{q_{GH_3^+}}}{\partial y} = -\frac{\partial (r^2 \overline{j_{GH_3^+}})}{\partial r} = \frac{1}{r^2}\frac{\partial}{\partial r}\left(r^2 \sum_{\nu = GH_3^+, VH_2^+, Na^+} \overline{D_{GH_3^+,\nu}} \frac{\partial q_\nu}{\partial r}\right) \tag{31a}$$

Here, the term on the left side corresponds to the rotational flux.

In the same manner, the following equations can be obtained for cationic valine and sodium ion:

$$u_y \frac{\partial \overline{q_{VH_2^+}}}{\partial y} = \frac{1}{r^2}\frac{\partial}{\partial r}\left(r^2 \sum_{\nu = GH_3^+, VH_2^+, Na^+} \overline{D_{VH_2^+,\nu}} \frac{\partial q_\nu}{\partial r}\right) \tag{31b}$$

$$u_y \frac{\partial \overline{q_{Na^+}}}{\partial y} = \frac{1}{r^2}\frac{\partial}{\partial r}\left(r^2 \sum_{\nu = GH_3^+, VH_2^+, Na^+} \overline{D_{Na^+,\nu}} \frac{\partial q_\nu}{\partial r}\right) \tag{31c}$$

The concentration of hydrogen ion can be calculated using the electroneutrality condition (Eq. 27).

For the resin surface, the following assumption is used:

7. Ion-exchange equilibria between the liquid and the resin phases are set up, and these relationships are described using constant ion-exchange selectivities, defined as

$$S_{GH_3^+} = \left.\frac{C_{H^+} q_{GH_3^+}}{C_{GH_3^+} q_{H^+}}\right|_{surface} \tag{32a}$$

$$S_{VH_2^+} = \left.\frac{C_{H^+} q_{VH_2^+}}{C_{VH_2^+} q_{H^+}}\right|_{surface} \tag{32b}$$

$$S_{Na^+} = \left.\frac{C_{H^+} q_{Na^+}}{C_{Na^+} q_{H^+}}\right|_{surface} \tag{32c}$$

These basic equations are solved under the boundary conditions suitable for the actual operation.

## Boundary Condition

In the same manner as in the previous study (12), the assumption of perfect mixing and a time mean procedure were employed for the bound-

ary condition at the inlet of the packed annular bed. [See Appendix in the previous paper (12).]

For amino acids,

$$\frac{C_T}{C_{T,0}} = \frac{y_{in} - y}{y_{in}} + \frac{1}{\Theta}\left[\alpha\left\{\exp(-\Theta) - \exp\left(-\Theta\frac{y}{y_{in}}\right)\right\} - \{1 - \alpha\exp(-\Theta)\}\left\{\exp\left(-\Theta\frac{y}{y_{in}} - 1\right)\right\}\right] \quad (0 < y \leq y_{in}) \tag{33a}$$

$$\frac{C_T}{C_{T,0}} = \frac{1}{\Theta}\left([\exp\{-(j-1)\Theta\} - \alpha\exp(-j\Theta)] \times \left[1 - \exp\left\{-\Theta\frac{y - (j-1)y_{in}}{y_{in}}\right\}\right] + [\exp\{-(j-2)\Theta\} - \alpha\exp\{-(j-1)\Theta\}] \times \left[\exp\left\{-\Theta\frac{y - (j-1)y_{in}}{y_{in}}\right\} - \exp(-\Theta)\right]\right) \quad [(j-1)y_{in} < y \leq jy_{in}, j = 2, 3, \ldots, 35) \tag{33b}$$

$$\frac{C_T}{C_{T,0}} = \frac{y - 35y_{in}}{y_{in}} + \frac{1}{\Theta}\left[\alpha\left\{\exp\left(-\Theta\frac{y - 35y_{in}}{y_{in}}\right) - 1\right\} - \{\exp(-34\Theta) - \alpha\exp(-35\Theta)\} \times \left\{\exp(-\Theta) - \exp\left(-\Theta\frac{y - 35y_{in}}{y_{in}}\right)\right\}\right] (35y_{in} < y \leq 36y_{in}) \tag{33c}$$

Here,

$$\Theta = y_{in}/u_y\tau_C \tag{34}$$

$$\alpha = \frac{1 - \exp(-35\Theta)}{1 - \exp(-36\Theta)} \tag{35}$$

and $\tau_C$ is the residence time in an inlet compartment.

For sodium acetate buffer,

$$C_{aT} = C_{aT,0} \tag{36a}$$

$$C_{Na^+} = C_{Na^+,0} \tag{36b}$$

Using the assumption of a closed vessel, the following equation is given as the boundary condition at the outlet of the bed $L$:

$$\left.\frac{\partial C_{gT}}{\partial x}\right|_{x=L} = \left.\frac{\partial C_{vT}}{\partial x}\right|_{x=L} = \left.\frac{\partial C_{aT}}{\partial x}\right|_{x=L} = \left.\frac{\partial C_{Na^+}}{\partial x}\right|_{x=L} = 0 \qquad (37)$$

Based on the continuity of the rotational direction of the annular bed, the following equations are obtained:

$$C_{gT}|_{y=0} = C_{gT}|_{y=2\pi R_d}; \quad \left.\frac{\partial C_{gT}}{\partial y}\right|_{y=0} = \left.\frac{\partial C_{gT}}{\partial y}\right|_{y=2\pi R_d} \qquad (38a)$$

$$C_{vT}|_{y=0} = C_{vT}|_{y=2\pi R_d}; \quad \left.\frac{\partial C_{vT}}{\partial y}\right|_{y=0} = \left.\frac{\partial C_{vT}}{\partial y}\right|_{y=2\pi R_d} \qquad (38b)$$

$$C_{aT}|_{y=0} = C_{aT}|_{y=2\pi R_d}; \quad \left.\frac{\partial C_{aT}}{\partial y}\right|_{y=0} = \left.\frac{\partial C_{aT}}{\partial y}\right|_{y=2\pi R_d} \qquad (38c)$$

$$C_{Na^+}|_{y=0} = C_{Na^+}|_{y=2\pi R_d}; \quad \left.\frac{\partial C_{Na^+}}{\partial y}\right|_{y=0} = \left.\frac{\partial C_{Na^+}}{\partial y}\right|_{y=2\pi R_d} \qquad (38d)$$

### Numerical Method

The model consists of simultaneous partial differential equations with 16 unknown variables. The equations were solved numerically using an iterative method with finite difference formulations. $x$, $y$, and $r$ axes were divided into 50, 150, and 25 grids for calculation, respectively. The adoption of these grid sizes was verified by agreement of the mass balance between the fed and recovered amounts of amino acids.

Dispersion coefficients in the liquid phase and diffusion coefficients in the resin phase were evaluated using a semiempirical equation by Ligny and Giddings (14) and correlation by Jones and Carta (15). The ion-exchange capacity and ion-exchange selectivities were measured using the technique of Dye et al. (16). Ion-exchange capacity was 2.338 mol/(kg-wet resin), and other parameters are listed in Table 2.

## EXPERIMENT FOR MODEL VERIFICATION

### Apparatus and Materials

Experiments for model verification were done using the CRAC apparatus with 36 nozzles and outlet ports which had been constructed in the previous study (12), with a slight change in the height of the annular bed

TABLE 2
Kinetic and Equilibrium Parameters

| Species | $E$ ($\times 10^{-7}$ m$^2$/s) | $\overline{D}$ ($\times 10^{-10}$ m$^2$/s) | $S$ (—) |
|---|---|---|---|
| Glutamic acid | 7.02 | 0.340 | 1.01 |
| Valine | 7.02 | 0.340 | 3.01 |
| Acetic acid | 7.00 | — | — |
| Sodium | 6.97 | 1.45 | 1.00 |
| Hydrogen | — | 10.1 | — |

to 300 mm in order to reduce the time for the attainment of steady state. In this apparatus the multichannel pump for effluent withdrawal and the effluent sampler are connected with a Tygon tube. The circumferential offset caused by the passage of the effluent in the withdrawal tube is incorporated in the numerical calculation by using the following equation:

$$y_{\text{sampler}} = y_{\text{outlet}} + u_y \frac{L_{\text{tube}}}{u_{\text{tube}}} \tag{39}$$

Here, $L_{\text{tube}}$ is the length of the tube and $u_{\text{tube}}$ is the linear velocity of the effluent in the tube.

A mixture of glutamic acid and valine (each concentration is 1 mol/m$^3$) as the feed solution and sodium acetate buffer (pH 5, sodium ion concentration is 10 mol/m$^3$) as the eluent were used. The feed solution contained sodium and acetate ions of the same concentration as the eluent. The annular bed was packed with a cation-exchange resin (Mitsubishi Kasei Co. UBK530, 0.22 mm in mean diameter, nominal degree of cross-linking 8%, $Na^+$ type).

After the steady state was attained (about 5–6 hours of operation), the effluent in each sampler was collected and analyzed using HPLC and a fluorescence spectrophotometer with the *o*-phthalaldehyde method to determine the amino acid concentration.

All chemicals were of special grade and were purchased from Wako Pure Chemicals Co., Japan.

All experiments were done at room temperature (23 ± 2 °C).

## RESULTS AND DISCUSSION

### Effect of Rotation Speed of Annular Bed

Calculated and experimental results are shown in Fig. 2 for a rotation speed of 0.1 deg/s and an interstitial liquid velocity of $1.34 \times 10^{-3}$ m/s.

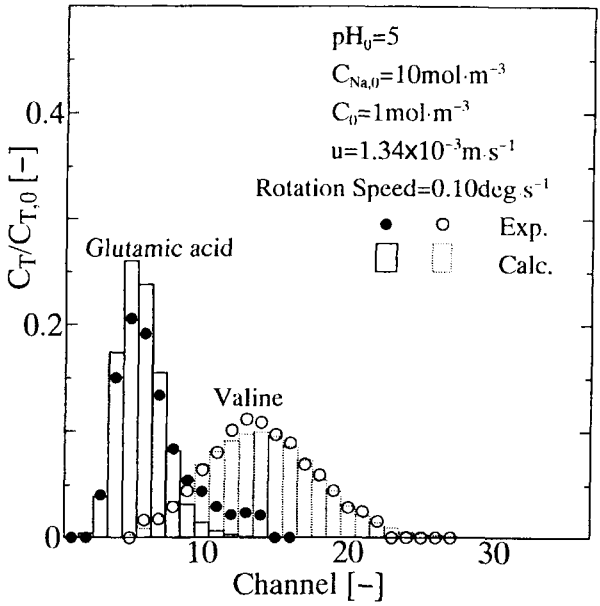


FIG. 2 Continuous separation of glutamic acid and valine.



The abscissa is the channel number of the effluent recovery ports. The first channel means the port just under the feeding nozzle, and the others are numbered along the rotational direction. The ordinate is the concentration of recovered amino acids nondimensionalized by the feed concentration. The filled and open circles mean the experimental values for glutamic acid and valine, respectively. The solid and broken bar graphs are the simulated values calculated using the presented model. Note that the simulated values are displayed in the following integral mean concentration for comparison with experimental values.

$$\frac{C_j}{C_0} = \frac{\int_{jy_{in}}^{(j+1)y_{in}} \frac{C}{C_0}\, dy}{\int_{jy_{in}}^{(j+1)y_{in}} dy} \tag{40}$$

For glutamic acid, the calculated peak height is slightly higher than the experimental value. The tendency is the same as that for column chromatographic results (13). This is considered to be due to the error in correlation of the diffusion coefficient of glutamic acid in the resin phase. On

the other hand, for valine, the simulated and experimental results agree fairly well.

Figure 3 shows the results for a rotation speed of 0.15 deg/s with all other parameters unchanged. In this case the calculated peak height for glutamic acid is also higher than the experimental value. For valine, the tendency of the peak shape is well simulated by the calculation, although the calculated one shifts to a lower angle by about one channel than the experimental one.

The results for a rotation speed of 0.05 deg/s are shown in Fig. 4. The experimental peak heights of both amino acids are about twice as high and the shapes are sharper than the results in Figs. 2 and 3, but the concentration overlap increases and good separation is not attained. Simulation describes these tendencies very well, although a slight shift in the peak of the valine occurs.



## Concentration Distributions in Annular Packed Bed

Figure 5 shows the simulated lines of constant concentration for the respective amino acids in the liquid phases under the condition of a rotation speed of 0.1 deg/s. The abscissa and the ordinate represent angular

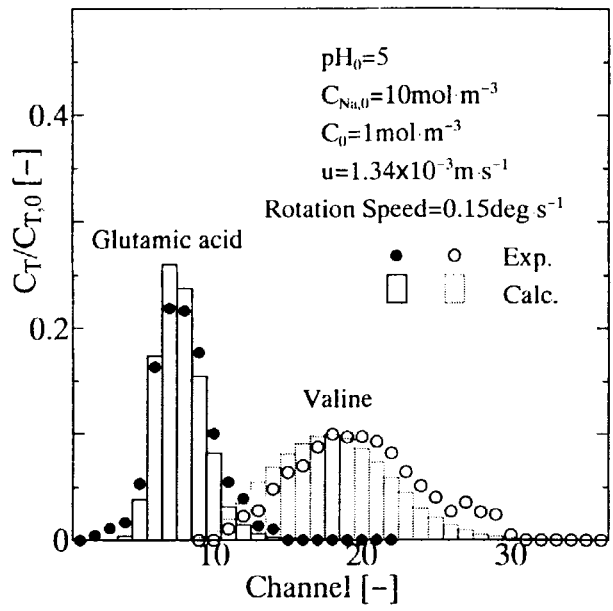


FIG. 3 Effect of rotation speed (1.5 times larger ω value).

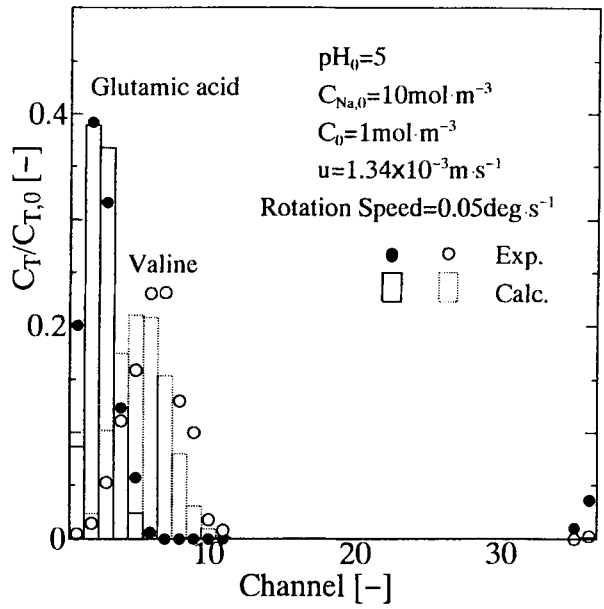


FIG. 4 Effect of rotation speed (half ω value).

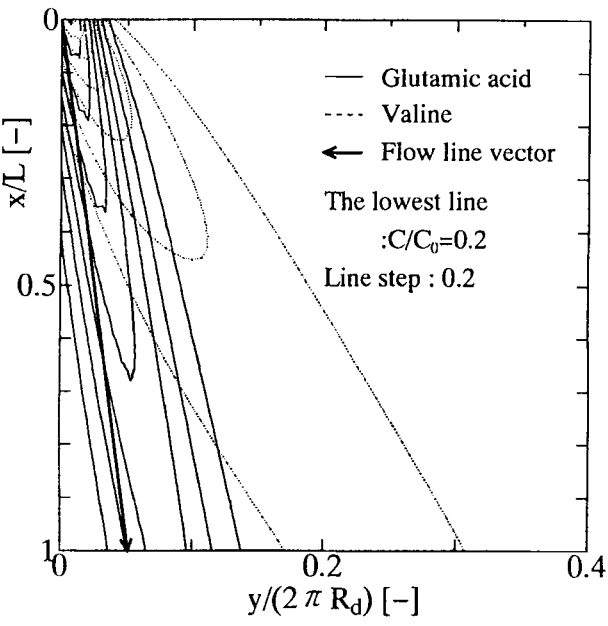


FIG. 5 Lines for constant concentration of amino acids in the liquid phase.

and axial coordinates nondimensionalized by the length of the annular circumference and the height of the annular bed, respectively. The solid arrow shows the flow line vector of the bulk liquid. It is clearly shown that both amino acids progress in inclined trajectories. The angle of inclination of the trajectory of glutamic acid is almost the same as that of the bulk liquid. On the other hand, the angle of valine is about three times larger than that of bulk liquid. Most of the glutamic acid exists in anionic form under this operational condition and is not substantially captured by the cation-exchange resin. On the contrary, some valine exists in cationic form. Hence valine is captured more by the resin and its elution speed is much slower. Therefore, it is carried to a larger angle by rotation of the annular bed than the bulk liquid. It is also shown that the concentration peaks for both amino acids become lower closer to the exit of the annular bed.

A similar chart for the resin phase is shown in Fig. 6. It is shown that the qualitative tendency of the concentration profile is as same as that for the liquid phase. A cross-sectional chart of concentration profiles of both amino acids in both phases at $x = L/5$ is shown in Fig. 7. The upper



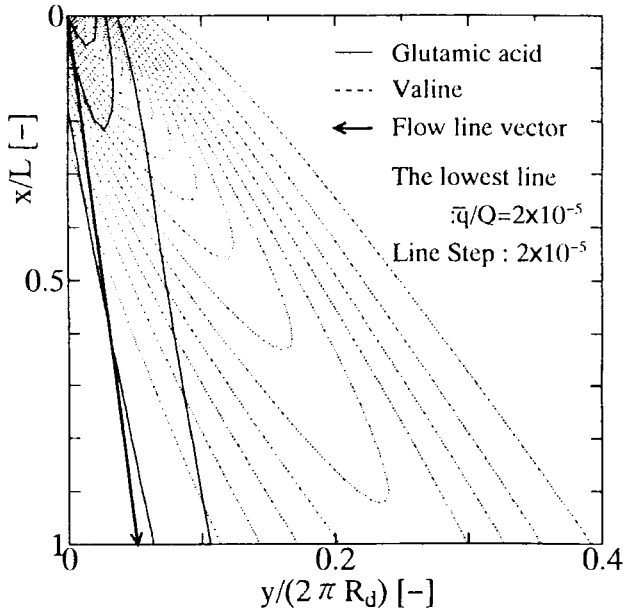


FIG. 6 Lines for constant concentration of amino acids in the resin phase.

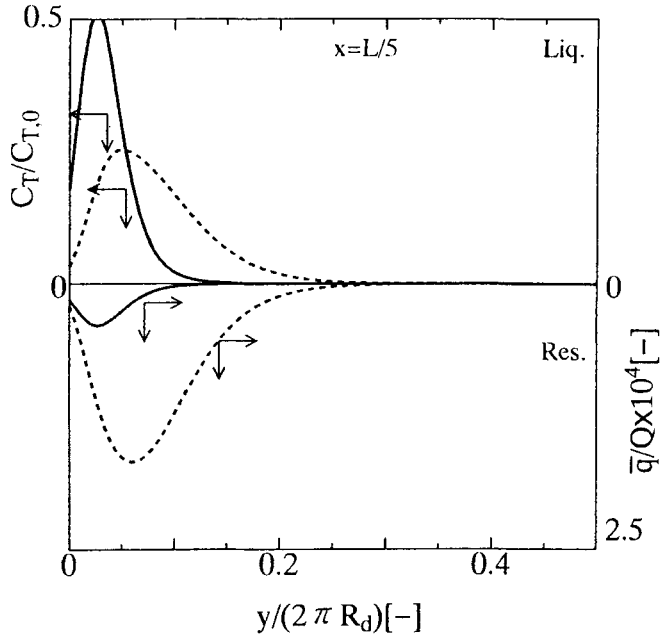


FIG. 7 Concentration distribution of amino acids at $x = L/5$.

and lower halves are for the liquid and resin phases, respectively. The maximum point of concentration in the resin phase exists at a slightly larger angle than that in the liquid phase. This is because amino acids in the resin phase are carried to a larger angle by the rotation due to the time lag of desorption caused by the intraparticle mass transfer resistance, as in the case of column chromatography (13).

## Concentration Distributions in Individual Resins

Figure 8 shows the calculated concentration distributions in individual ion-exchange resins at several circumferential angles in the annular bed for a rotation speed of 0.1 deg/s. The axial position is fixed at $x = L/5$. The angular coordinate $\theta$ is defined as $\theta = 180y/\pi R_d$. The abscissa of each figure is the radial coordinate of the ion-exchange resin nondimensionalized by its own radius, in which 0 and 1 mean the center and the surface, respectively. It must be noted that the maximum of the volume mean concentration exists between (a) and (b) for glutamic acid and (b) and (c) for valine, respectively, in Fig. 8. The tendency of the distribution changes between the resins in smaller and larger angles than the peak

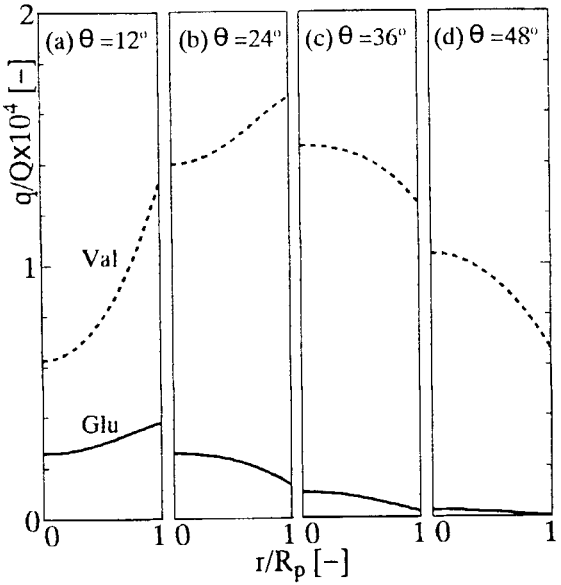


FIG. 8 Concentration distributions in individual resin at $x = L/5$.

position, showing the domination of capture and desorption, respectively. It is also certified that a large concentration gradient exists, and consequently a large mass transfer resistance exists in the resin phase, especially for valine.

## Effect of Interstitial Liquid Velocity

Figure 9 shows the experimental and simulated results for a rotation speed of 0.1 deg/s and an interstitial liquid velocity of $2.68 \times 10^{-3}$ m/s, twice that in Figs. 2–4. The peak positions of both amino acids in Fig. 9 are almost the same as that in Fig. 4. This is because the elution angle in CRAC is roughly proportional to both the rotation speed $\omega$ and the residence time of liquid in the packed bed $\tau$ [so-called "equilibrium model" (2, 17, 18)]. Note that the product values $\omega\tau$ are the same in these two figures.

Figures 10 and 11 also show the results at twice the interstitial liquid velocity for rotation speeds of 0.2 and 0.3 deg/s. The product values $\omega\tau$ of both are the same as those of Figs. 2 and 3, respectively. The peak positions of both amino acids in these figures follow the equilibrium model.

However, it is also shown that the shapes of the peaks at smaller residence time, i.e., larger interstitial velocity, are broader than that at larger

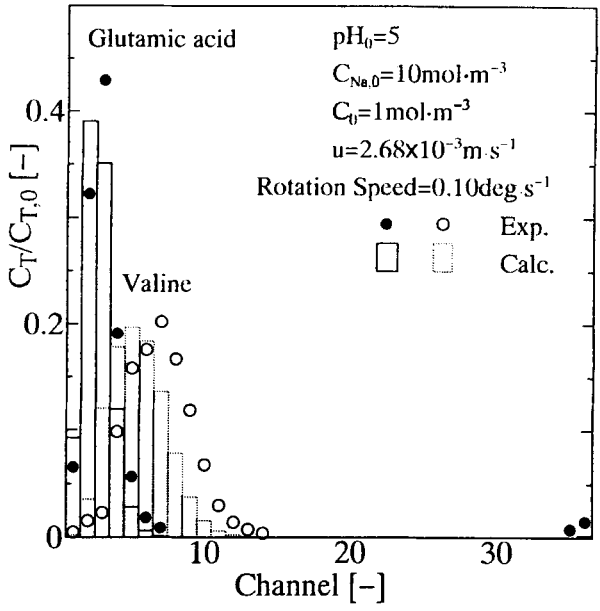


FIG. 9 Effect of liquid velocity ($\omega\tau$ value is the same as in Fig. 4).

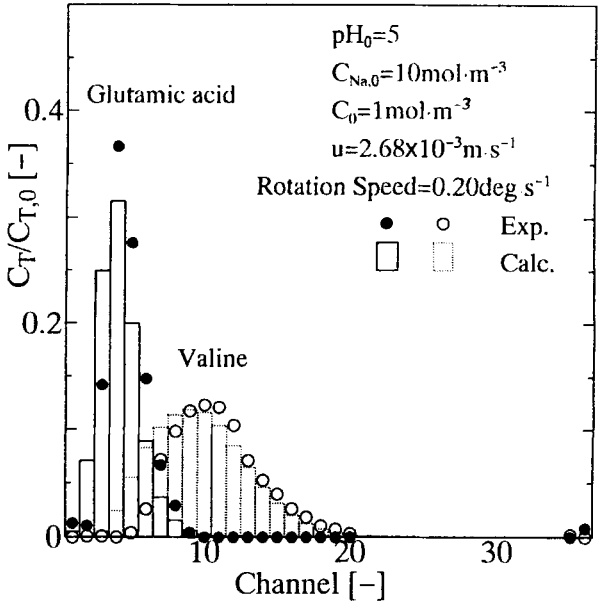


FIG. 10 Effect of liquid velocity ($\omega\tau$ value is the same as in Fig. 2).

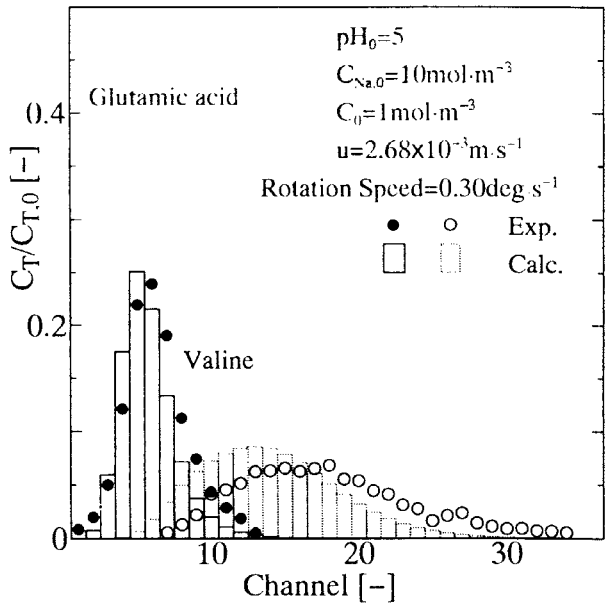


FIG. 11 Effect of liquid velocity ($\omega\tau$ value is the same as in Fig. 3).



residence time. This is because the deviation from the ion-exchange equilibrium increases with interstitial liquid velocity. The deviation reduces the ideality of the chromatographic separation and consequently broadens the peak shapes.

## CONCLUSIONS

The separation process of amino acids using continuous rotating annular ion-exchange chromatography was numerically simulated with a newly constructed mathematical model. The model closely simulated the separation experiment with the amino acids.

The effects of rotation speed and interstitial liquid velocity on resolution of the amino acids were discussed. It was shown theoretically and experimentally that the peak shapes became broader at larger interstitial liquid velocity due to increased deviation from ion-exchange equilibrium.

By adding the pH or ionic strength distribution at the circumference of the annular bed using various eluents, the gradient elution method (6, 19) can be applied to the apparatus used in this work. The present model is applicable over such a range of wide operation conditions (13) that it may be applied to the gradient elution method with a slight extension.

## NOMENCLATURE

| | |
|---|---|
| $C$ | concentration in liquid phase (mol/m$^3$) |
| $\overline{D}$ | diffusion coefficient in resin phase (m$^2$/s) |
| $E$ | dispersion coefficient (m$^2$/s) |
| $\mathcal{F}$ | Faraday constant (coulomb/mol$^{-1}$) |
| $H$ | volume ratio of liquid and solid phases (—) |
| $\bar{j}$ | ionic flux in resin phase (mol/m$^2$·s) |
| $j$ | channel number (—) |
| $K$ | dissociation constants (mol/m$^3$) |
| $K_w$ | ionic product of water (mol$^2$/m$^{-6}$) |
| $L$ | height of annular packed bed (m) |
| $L_{tube}$ | length of connecter tube between withdrawal pump and sampler (m) |
| $Q$ | ion-exchange capacity (mol/m$^3$) |
| $q$ | concentration in resin phase (mol/m$^3$) |
| $\bar{q}$ | mean concentration in resin phase (mol/m$^3$) |
| $\mathcal{R}$ | gas constant (J/mol·K) |
| $r$ | radial coordinate in resin phase (m) |
| $R_d$ | radius of annular packed bed (m) |
| $R_p$ | radius of resin particle (m) |
| $S$ | ion-exchange selectivity (—) |
| $\mathcal{T}$ | temperature (K) |
| $t$ | time (s) |
| $u$ | interstitial liquid velocity (m/s) |
| $u_{tube}$ | liquid velocity in connecter tube between withdrawal pump and sampler (m/s) |
| $u_y$ | linear velocity of rotation (m/s) |
| $V$ | volume (m$^3$) |
| $V_r$ | volume of ion exchange resin particle (m$^3$) |
| $W$ | width of elution peak (—) |
| $x$ | axial coordinate (m) |
| $y$ | circumferential coordinate (m) |
| $y_{in}$ | width of inlet chamber (m) |
| $z$ | net charge of ionic species (—) |

### *Greeks*

| | |
|---|---|
| $\alpha$ | nondimensional number defined in Eq. (35) (—) |
| $\epsilon$ | void fraction (—) |
| $\Theta$ | nondimensional number defined in Eq. (34) (—) |
| $\theta$ | angular offset from the feed inlet nozzle (deg) |
| $\tau$ | residence time in annular bed (s) |

| | |
|---|---|
| $\tau_C$ | residence time in inlet compartment (s) |
| $\psi$ | electric potential (V) |
| $\omega$ | rotation speed (deg/s) |

### *Subscripts*

| | |
|---|---|
| a | acetic acid |
| g | glutamic acid |
| *j* | *j*th channel |
| n | sodium |
| peak | elution peak |
| r | resin phase |
| T | total |
| v | valine |
| x | axial direction |
| y | circumferential direction |
| 0 | concentration in feed solution or eluent |

## REFERENCES


1. A. J. P. Martin, *Disc. Faraday Soc.*, *7*, 332 (1949).
2. J. C. Giddings, *Anal. Chem.*, *34*, 37 (1962).
3. J. B. Fox, R. C. Calhoun, and W. J. Eglinton, *J. Chromatogr.*, *43*, 48 (1969).
4. J. B. Fox, *Ibid.*, *43*, 55 (1969).
5. R. A. Nicholas and J. B. Fox, *Ibid.*, *43*, 61 (1969).
6. J. P. De Carli, G. Carta, and C. H. Byers, *AIChE J.*, *36*, 1220 (1990).
7. Y. Takahashi and S. Goto, *J. Chem. Eng. Jpn.*, *24*, 121 (1991).
8. Y. Takahashi and S. Goto, *Ibid.*, *24*, 460 (1991).
9. G. F. Bloomingburg, J. S. Bauer, and G. Carta, *Ind. Eng. Chem. Res.*, *30*, 1061 (1991).
10. Y. Takahashi and S. Goto, *J. Chem. Eng. Jpn.*, *25*, 403 (1992).
11. F. Helfferich, *Ion Exchange*, p. 250, McGraw-Hill, New York, 1962.
12. T. Yonemoto, A. Kitakawa, S. N. Zheng, and T. Tadaki, *Sep. Sci. Technol.*, *28*, 2587 (1993).
13. A. Kitakawa, T. Yonemoto, and T. Tadaki, *Trans. Inst. Chem. Eng., Part C*, *72*, 201 (1994).
14. C. L. Ligny, *Chem. Eng. Sci.*, *25*, 1177 (1970).
15. I. L. Jones and G. Carta, *Ind. Eng. Chem. Res.*, *32*, 117 (1993).
16. R. S. Dye, J. P. De Carli, and G. Catra, *Ibid.*, *29*, 849 (1990).
17. P. C. Wankat, *AIChE J.*, *23*, 859 (1977).
18. P. C. Wankat, *Sep. Sci. Technol.*, *19*, 801 (1984).
19. F. D. Antia and C. Horvath, *Ber. Bunsenges. Phys. Chem.*, *93*, 961 (1989).


*Received by editor February 22, 1995*